Smart Structures and Systems, *Vol. 22, No. 3 (2018) 277-290*
DOI: https://doi.org/10.12989/sss.2018.22.3.277

Progressive damage detection of thin plate structures using wavelet finite element model updating

Wen-Yu He[1a], Songye Zhu[*2] and Wei-Xin Ren[1b]

[1]*Department of Civil Engineering, Hefei University of Technology, Hefei, 230009, China*
[2]*Department of Civil and Environmental Engineering, The Hong Kong Polytechnic University, Hung Hom, Kowloon, Hong Kong*

(Received February 6, 2018, Revised April 27, 2018, Accepted June 30, 2018)

Abstract. In this paper, wavelet finite element model (WFEM) updating technique is employed to detect sub-element damage in thin plate structures progressively. The procedure of WFEM-based detection method, which can detect sub-element damage gradually, is established. This method involves the optimization of an objective function that combines frequencies and modal assurance criteria (MAC). During the damage detection process, the scales of wavelet elements in the concerned regions are adaptively enhanced or reduced to remain compatible with the gradually identified damage scenarios, while the modal properties from the tests remains the same, i.e., no measurement point replacement or addition are needed. Numerical and experimental examples were conducted to examine the effectiveness of the proposed method. A scanning Doppler laser vibrometer system was employed to measure the plate mode shapes in the experimental study. The results indicate that the proposed method can detect structural damage with satisfactory accuracy by using minimal degrees-of-freedoms (DOFs) in the model and minimal updating parameters in optimization.

Keywords: progressive damage detection; thin plate; wavelet finite element; model updating

1. Introduction

Thin plate is an important type of structural components in civil and mechanical structures and detecting its damage in early stage will be essential in future monitoring and maintenance. Vibration-based damage detection methods using the damage-induced changes in structural dynamic characteristics have been extensively studied in recent years (Yan *et al.* 2007, Fan and Qiao 2011). Based on the dependence on structure modeling, these methods can be classified into model-free and model-based types. The former is regarded as more appealing and efficient by several scholars (Rucka and Wilde 2006, Beheshti-Aval *et al.* 2011). However, some inherent limitations, such as the inability to estimate damage severity and the need for a dense network of sensors to accurately locate damage, prevent the extensive application of model-free methods (Antonio and Erin 2014). Thus, model-based methods, particularly finite element model (FEM) based methods, have been eliciting widespread attention.

Cornwell *et al.* (1999) defined a damage index as the ratio of the normalized modal strain energy (MSE) of plate structure in undamaged and damaged states. Numerical results indicated that the index could provide accurate information about the damage location. Lee and Shin (2002) developed a reduced-domain damage identification method in which the damage-free zones were removed iteratively from the original domain using the modal data in the intact state and the frequency response functions in the damaged state. Yam *et al.* (2002) presented two damage indices related to strain frequency response function and curvature mode shapes to locate damage and provided recommendations for selecting damage indices in different cases. Wu and Law (2004) used the uniform load surface curvature change to locate damages and only the first few frequencies and mode shapes were required. Bayissa and Haritos (2007) derived several damage indices from the bending moment response power spectral density to detect and locate single and multiple damages in plate structures. By taking advantage of the recent advancement in moving scanning technology, Hu and Wu (2009) established a scanning damage index related to MSE by moving indices acquired from a local area throughout the entire structure; the authors used the index to localize and quantify damage in a plate. With the variation of modal flexibility and artificial neural network technique, Kazemi *et al.* (2010) proposed a two-stage damage detection procedure, i.e., localize the probable damaged regions and then estimate the severity of identified regions for plate structures. Fan and Qiao (2012) presented a plate damage detection method that combines two factors derived from the elemental MSE, i.e., damage location factor matrix and damage severity correction factor. This method consisted of three steps: sensitive mode selection, damage localization, and damage quantification. Fu *et al.* (2013) identified damages in plate through response sensitivity-based model updating in the time domain, in which only short time histories of a few number of measurement points were needed.

An interesting observation is that the application of

*Corresponding author, Associate Professor
E-mail: ceszhu@polyu.edu.hk
[a] Ph.D.
E-mail: wyhe@hfut.edu.cn
[b] Professor
E-mail: renwx@hfut.edu.cn

ISSN: 1738-1584 (Print), 1738-1991 (Online)

FEM updating technique was widely applied in beam damage detection (Teughels *et al.* 2002, Jaishi and Ren 2005, Fang *et al.* 2008), but was very limited in plate structures. One main reason is that compared to 1D structures, the FEM updating of 2D plate structures involves more degree-of-freedoms (DOFs) in the model and more parameters to be optimized, which would increase the computation amount dramatically and even make the solutions ill-conditioned and non-unique.

He and Zhu (2013) highlighted that a multi-scale FEM with high resolution in damage regions and relatively low resolution elsewhere is favorable to obtain acceptable damage detection accuracy by using the least number of DOFs and updating parameters. They presented a progressive method to detect beam damage based on wavelet FEM (WFEM) (Amaratunga and Sudarshan 2006, He and Ren 2012, Li and Chen 2014) updating. The resolutions of the model change according to the progressively identified damage scenarios, i.e., using a low-resolution model to localize the probable damage regions and then refine the model locally only in the suspected regions to acquire accurate damage detection results.

Later on, WFEM combined with modal strain energy (MSE) was adopted to localize and quantify damage adaptively in 1D beam (He *et al.* 2014). Thanks to the multi-resolution property of wavelet, re-meshing the structure when adjusting the modelling scale is not required in WFEM. Therefore the challenges associated with hanging nodes in plate structures can be avoided (Becker and Braack 2000, Biboulet *et al.* 2013). However, these MSE based methods require more sensors to be installed in the suspected damage regions during the damage detection process. In particular, the need for the measurement of rotational DOFs in mode shapes makes their implementation very difficult, if not impossible, in real applications. Moreover, the method is highly sensitive to noise because only mode shapes are adopted. In view of this, model updating based progressive damage detection method which can operate efficiently in terms of the DOFs in WFEM and updating parameters in optimization (Zhu e*t al.* 2013, He and Zhu 2013) has been extended from 1D beam to 2D thin plate in this study. Firstly, taking the tensor product of cubic Hermite multi-wavelets as elemental shape function, the multi-scale dynamic equation of thin plate structures for obtaining modal parameters was derived. Sub-element damage could be detected progressively through multi-scale model updating according to the measured modal properties. During the damage detection process, the scales of the wavelet elements in the regions of concern were adaptively enhanced or reduced to remain compatible with the gradually identified damage; the test modal information remained the same in the progressive process, i.e., no sensors replacement or new sensors were needed. Compared to traditional FEM, it involves less number of DOFs and updating parameters. Numerical and experimental examples were analyzed to verify the effectiveness of the proposed method.

2. Multi-scale WFEM

WFEM combines the FEM framework with wavelet functions. It uses the scaling or wavelet functions as elemental shape functions and serves the theoretical basis of the progressive damage detection method. Various types of wavelet elements have been constructed for plates using different wavelets, such as spline wavelets (Han *et al.* 2006), B-spline wavelets (Xiang *et al.* 2008), Daubechies wavelets (Diaz *et al.* 2009), Hermite wavelets (Quraishi and Sandeep 2013), trigonometric wavelets(He and Ren 2013), and so on.

He and Zhu (2014) used the second-generation cubic Hermite multi-wavelet (Wang and Wu 2013) element with superior localization feature and favorable compatibility with traditional FEM to localize and quantify plate damages. The 2D second-generation cubic Hermite multi-wavelet and corresponding multi-scale dynamic equation for obtaining modal parameters are briefly introduced in this section. More details were presented by He and Zhu (2014).

The scaling function of the 2D cubic Hermite wavelets of scale j, $\bar{\mathbf{\Phi}}_j = \{\bar{\mathbf{\Phi}}_j^1, \bar{\mathbf{\Phi}}_j^2, \bar{\mathbf{\Phi}}_j^3, \bar{\mathbf{\Phi}}_j^4\}$, consists of four functions as follows (Wang and Wu 2013, He and Zhu 2014)

$$\bar{\mathbf{\Phi}}_j^1(x,y) = \mathbf{\Phi}_j^1(x) \times \mathbf{\Phi}_j^1(y) \tag{1a}$$

$$\bar{\mathbf{\Phi}}_j^2(x,y) = \mathbf{\Phi}_j^1(x) \times \mathbf{\Phi}_j^2(y) \tag{1b}$$

$$\bar{\mathbf{\Phi}}_j^3(x,y) = \mathbf{\Phi}_j^2(x) \times \mathbf{\Phi}_j^1(y) \tag{1c}$$

$$\bar{\mathbf{\Phi}}_j^4(x,y) = \mathbf{\Phi}_j^2(x) \times \mathbf{\Phi}_j^2(y) \tag{1d}$$

where $\mathbf{\Phi}_j$ is the scaling function of 1D wavelet. These functions stand for the displacement, x-direction difference, y-direction difference, and diagonal difference of the displacement field, respectively. The corresponding 2D wavelet functions $\bar{\mathbf{\Psi}}_j$ of scale j is

$$\bar{\mathbf{\Psi}}_j = \bar{\mathbf{\Phi}}_{j+1} \tag{2}$$

The 2D wavelets at the scale j = 1 are shown in Fig.1.

By using the 2D multi-wavelets $\bar{\mathbf{\Phi}}_j$ as shape function and translating the corresponding coordinate of a thin plate element with dimensions $l_x \times l_y$ into standard solving domain, the unknown displacement field function $w(\xi,\eta)$ can be expressed as

$$w(\xi,\eta) = \bar{\mathbf{\Phi}}_0 \mathbf{a}_0 + \sum_{n=0}^{j-1} \bar{\mathbf{\Psi}}_n \mathbf{b}_n = \bar{\mathbf{\Phi}}_j \mathbf{q}_j \tag{3}$$

where ξ and η denote the local coordinates, $\bar{\mathbf{\Phi}}_0$ represents the scaling functions at scale 0, $\bar{\mathbf{\Psi}}_j = [\bar{\mathbf{\Phi}}_0\ \bar{\mathbf{\Psi}}_0\ \bar{\mathbf{\Psi}}_1 \cdots \bar{\mathbf{\Psi}}_{j-1}]$ represents the wavelet functions at

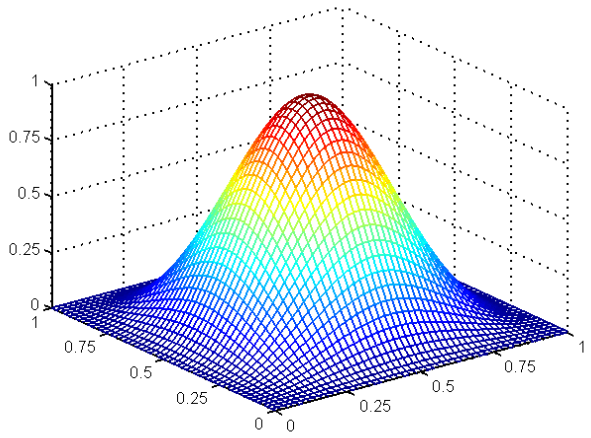

(a) Scaling function $\bar{\mathbf{\Phi}}_1^1$

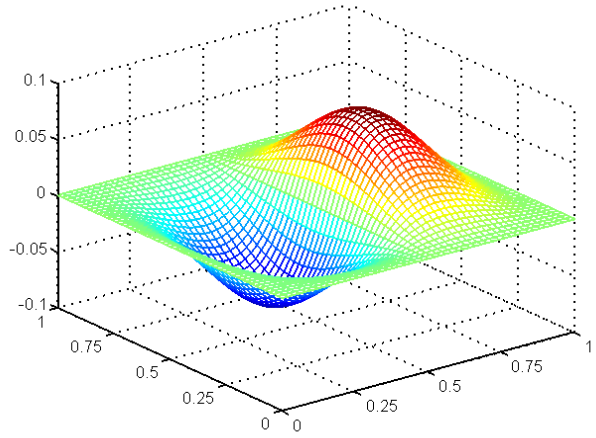

(b) Scaling function $\bar{\mathbf{\Phi}}_1^2$

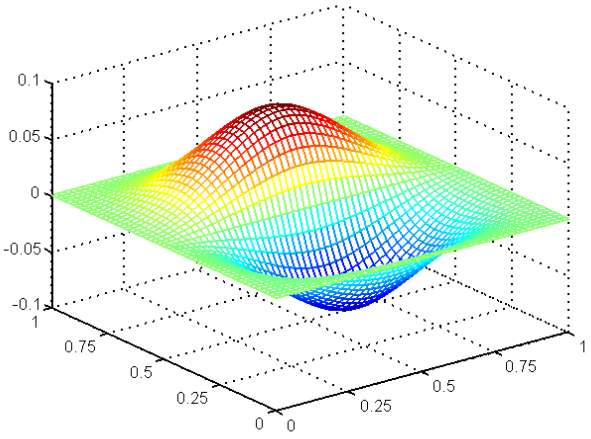

(c) Scaling function $\bar{\mathbf{\Phi}}_1^3$

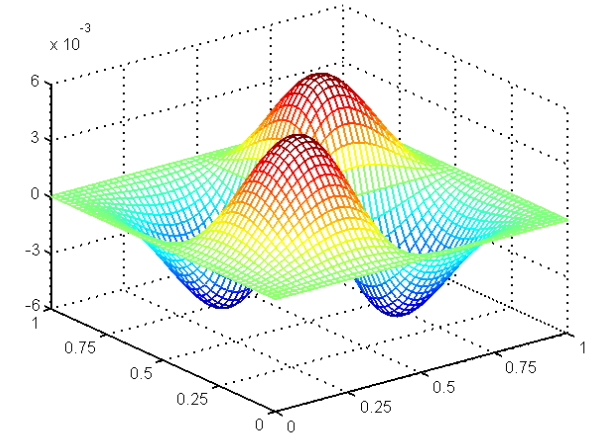

(d) Scaling function $\bar{\mathbf{\Phi}}_1^4$

Fig. 1 2D tensor products of cubic Hermite functions (He and Zhu 2014)

scale j and $\mathbf{q}_j$ is the undetermined vector of the wavelet coefficients (i.e., the coordinates corresponding to wavelet DOFs). The mode shapes obtained in the vibration test, which are expressed in the physical coordinate, can be conveniently converted into wavelet DOFs by exploiting the interpolation properties of the adopted multi-wavelets.

Then the wavelet formulations for the modal analysis of elastic thin plates can be expressed as follow

$$(\mathbf{K}_j - \lambda \mathbf{M}_j)\mathbf{q}_j = 0 \tag{4}$$

where $\mathbf{K}_j$ and $\mathbf{M}_j$ are the element stiffness and mass matrices at scale j, respecitvely

$$\mathbf{M}_j = l_x l_y \rho t \mathbf{\Gamma}_1^{j,0,0} \otimes \mathbf{\Gamma}_2^{j,0,0} \tag{5}$$

$$\begin{aligned} \mathbf{K}_j = D[&\mathbf{\Gamma}_1^{j,2,2} \otimes \mathbf{\Gamma}_2^{j,0,0} + \mu \mathbf{\Gamma}_1^{j,0,2} \otimes \mathbf{\Gamma}_2^{j,2,0} \\ &+ \mathbf{\Gamma}_1^{j,0,0} \otimes \mathbf{\Gamma}_2^{j,0,0} + 2(1-\mu)\mathbf{\Gamma}_1^{j,1,1} \otimes \mathbf{\Gamma}_2^{j,1,1}] \end{aligned} \tag{6}$$

where λ is the vibration eigenvalue, $D = Et^3/[12(1-\mu^2)]$ is the flexural rigidity, μ is the Poisson's ratio. More details of integrals $\mathbf{\Gamma}_s^{j,f,g}$ ($f, g = 0, 1, 2; s = 1, 2$) can be found in He and Zhu (2014).

As indicated in Section 1, the element scales of WFEM change dynamically according to the progressively identified damage scenarios; the convenient changes in scale are crucial in progressive damage detection. In the lifting or lowering procedure between scales, the sub-matrices of the current scale can be retained, and only a few rows and columns need to be added or deleted. Notably, the support region of the 2D wavelet at scale j + 1 is only a quarter of scale j. This favorable localization characteristic helps develop the progressive damage detection method. In the multi-scale model, an original region can be refined to four equal sub-regions by enhancing the scale by one.

Furthermore, the bi-cubic Hermite wavelet functions of scale 0 are the same as the polynomial shape functions of the Bogner-Fox-Schmidt plate element (Bogner *et al.* 1995), which is widely used in the traditional FEM. Therefore, the presented WFEM can seamlessly connect to

the traditional finite element or even refine elements in traditional FEM. Considering the fact that most existing structural models are built using traditional FEM, this feature of cubic Hermite WFEM is a prominent advantage that makes the proposed progressive damage detection method more acceptable.

3. Progressive updating of WFEM

The model updating based progressive damage detection method for plate structures is described in this section. FEM updating is widely used in damage detection by minimizing the discrepancy between the test data and model simulation.

3.1 Updating parameters and objective function

In this study, structural damage is assumed to be the flexural rigidity reduction in a sub-element region. Thus the damage index is defined by the relative variation of sub-element flexural rigidity

$$DS_s = 1 - D_d^s / D_u^s \tag{7}$$

in which D_u^s and D_d^s are flexural rigidity before and after damage, respectively; the subscripts u and d denote the undamaged and damaged states, respectively. Given that damage size is assumed to be only part of an element rather than an entire element, the primary multi-scale and localization characteristics of WFEM can be fully utilized.

The optimization problem aims to minimize the difference between the experimental and analytical modal properties by updating sub-element flexural rigidity. The measured natural frequencies and modal assurance criterion (MAC), which are commonly adopted in model updating, are also utilized in the objective function of this study.

$$\begin{aligned}\min\ J(\mathbf{p}) = &\sum_{i=1}^{n}\alpha_i[(\frac{\lambda_{ai}(\mathbf{p})-\lambda_{ai}^0}{\lambda_{ai}^0})-(\frac{\lambda_{ei}^d-\lambda_{ei}^u}{\lambda_{ei}^u})]^2 \\ &+\sum_{i=1}^{n}\beta_i[sqrt\left(MAC_{ai}(\mathbf{p})\right)-sqrt(MAC_{ei})]^2\end{aligned} \tag{8}$$

$$\lambda_{ai} = (2\pi f_{ai})^2 \tag{9a}$$

$$\lambda_{ei} = (2\pi f_{ei})^2 \tag{9b}$$

$$MAC_{ai} = \frac{[\phi_{ai}^T(\mathbf{p})\phi_{ai}^0]^2}{[\phi_{ai}^T(\mathbf{p})\phi_{ai}(\mathbf{p})][(\phi_{ai}^0)^T\phi_{ai}^0]} \tag{10a}$$

$$MAC_{ei} = \frac{[(\phi_{ei}^u)^T\phi_{ei}^d]^2}{[(\phi_{ei}^u)^T\phi_{ei}^d][(\phi_{ei}^u)^T\phi_{ei}^d]} \tag{10b}$$

where the vector $\mathbf{p} \in R^n$ represents the set of updating parameters; superscripts 0, u and d denote the initial, undamaged and damaged states, respectively; f_{ai} and f_{ei} are the analytical and experimental natural frequencies of the i^{th} mode, respectively; ϕ_{ai} and ϕ_{ei} are the analytical and experimental mode shapes of the i^{th} mode, respectively; α_i and β_i are the weighting factors of the i^{th} mode, which are usually assigned according to their importance and measurement accuracy in experiments. In the following numerical and experimental study, they were all set to 1.

For the numerical study, considering that the initial state (denoted by 0) of the WFEM is assumed to be the same as the undamaged state (denoted by u), the objective function can be simplified as

$$\min J(\mathbf{p}) = \sum_{i=1}^{n}\alpha_i[\frac{\lambda_{ai}(\mathbf{p})-\lambda_{ei}}{\lambda_{ei}}]^2 + \sum_{i=1}^{n}\beta_i[sqrt(MAC_i)-1]^2 \tag{11}$$

$$MAC_i = \frac{(\phi_{ai}^T\phi_{ei})^2}{(\phi_{ai}^T\phi_{ai})(\phi_{ei}^T\phi_{ei})} \tag{12}$$

3.2 Progressive damage detection

By using the appealing multi-scale characteristics of WFEM, a progressive damage detection strategy can be developed for plate structures. Fig. 2 presents the flowchart of this damage detection scheme. The detailed procedure is described as follows.

Step 1: Install sensors on the concerned plate and measure its frequencies and mode shapes, and then calculate the MACs. Only the magnitudes of the mode shapes at DOFs coincident with measurement locations are adopted.

Step 2: Select and initialize the updating parameters, update a relatively low-scale WFEM, and estimate the occurrence and approximate location of damage (if any).

Step 3: Refine the WFEM in the suspected region accordingly by adding high-scale wavelet terms. Select the updating parameters in the suspected region only, and update the lifted-scale WFEM. Consequently, the damage can be localized and quantified with improved accuracy.

Step 4: Check the convergence of the results, and stop if the difference is smaller than a prescribed threshold. Otherwise, repeat Step 3.

During the damage detection process, the updating parameters are adaptively selected according to the gradually identified damage conditions and limited to the suspected regions only. Thus, the computation cost in the optimization process can be reduced considerably. Furthermore, only WFEM is adaptively changed, and no additional requirements, such as installing more sensors in the suspected damage regions, and measurement of rotational DOFs in mode shapes, are necessary in the modal test. Therefore, the method proposed in this paper is more practical, compared to that presented by He and Zhu (2014).

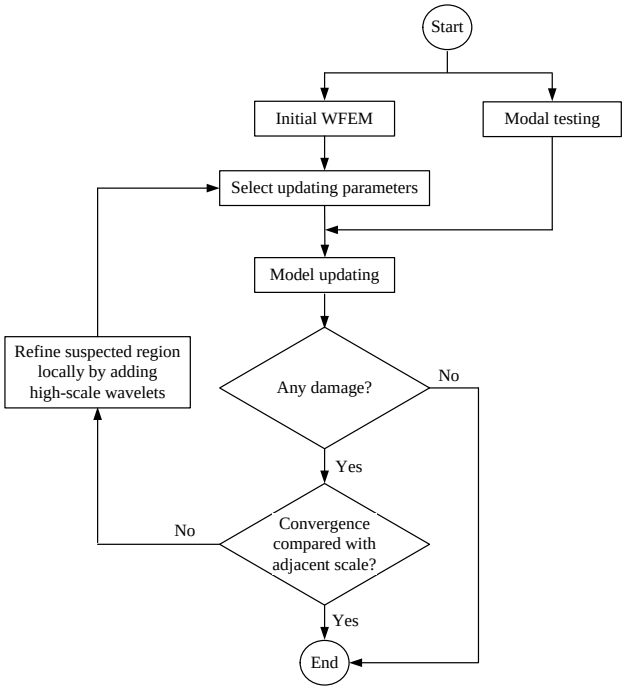

Fig. 2 The progressive WFEM updating scheme

4. Numerical study

A thin plate simply supported on four corners (Fig. 3) with different damage scenarios (as summarized in Table 1) was simulated to demonstrate the effectiveness of the proposed damage detection method. The physical material properties were: dimensions 700 mm × 500 mm × 3 mm, elastic modulus $E = 68.9$ Gpa , Poisson's ratio $\mu = 0.27$, and density $\rho = 2700$ Kg/m^3 . Considering that only the lower modes can be measured in real tests and the difficulty in the measurement of rotational DOFs, only the first four frequencies and the vertical DOFs in the mode shapes at the 44 measurement locations (Fig. 3) were used during the whole damage detection process. Densely-meshed traditional FEMs were used to simulate the damaged structures and extract modal properties.

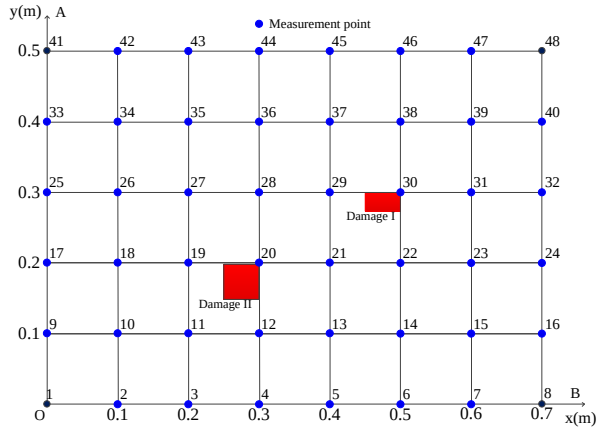

Fig. 3 Thin plate in the numerical study

Table 1 Damage scenarios considered in the numerical simulations of the plate

Damage Scenarios		Damage	
		Region(m)	Severity (%)
Case 1	Damage I	[0.450, 0.500] × [0.275, 0.300]	30
Case 2	Damage I	[0.450, 0.500] × [0.275, 0.300]	30
	Damage II	[0.250, 0.300] × [0.150, 0.200]	20

The noise effect was taken into account in the numerical simulations by adding uncorrelated random uncertainties to the theoretical frequencies and mode shapes. The noisy mode shape is represented by

$$\bar{\varphi}_{i,r} = \varphi_{ir}(1+\eta\zeta_{ir}) \tag{13}$$

where $\bar{\varphi}_{i,r}$ and φ_{ir} are the "measured" and accurate mode shape components of the i^{th} mode at the r^{th} DOF, respectively; η is the measurement error level considered; and ζ_{ir} is zero-mean Gaussian random variables. The frequencies contaminated with noise were defined similarly. In this study, 0.5% artificial random error was introduced in the frequencies and mode shapes.

Case 1 involved a single damage in the region [0.45, 0.5] ×[0.275, 0.3] with 30% severity. Figs. 4 and 5 show the detection process and the corresponding results, respectively. The entire detection process of Case 1 consisted four stages. In Stage 1, the plate was divided into 35 (7×5) wavelet elements at scale 0, that is, the displacement was approximated in wavelet space F0. The damage indices of the 35 elements were obtained by minimizing the objective function as defined in Eq. (11); the results were plotted in Fig. 5(a). The region [0.4, 0.5]×[0.2, 0.3] (denotes as ABCD) was a potential damage region, although the damage severity was not estimated accurately due to the low-scale model. In Stage 2, wavelets of scale 0 were added to the potential damage region (ABCD) of the WFEM to lift the approximation space from F0 to F1. Four damage indices associated with the four equal sub-regions divided from region ABCD (Fig. 4) were regarded as updating parameters. The significantly reduced number of updating parameters greatly minimized the corresponding computation amount. With the estimated damage severities in Stage 1 as initial values, the optimization process was implemented again to acquire more precise results. The results shown in Fig. 5(b) indicate that the region [0.45, 0.5] × [0.25, 0.3] was more likely a damaged region than the other three, which means the damage was localized in a small region. Similar refinements were applied in the progressively identified potential damage regions, and the optimization processes were implemented accordingly. Hence, more accurate estimations of the damage location and severity were obtained (Figs. 5(c) and 5(d)). Stage 3 and Stage 4 presented almost the same detection results that were close to the real value. For example, the damage region of [0.45, 0.5]×[0.4275, 0.3] was identified in both Stages 3 and 4, with the average damage severity equal to 29.6% and 30.1%, respectively.

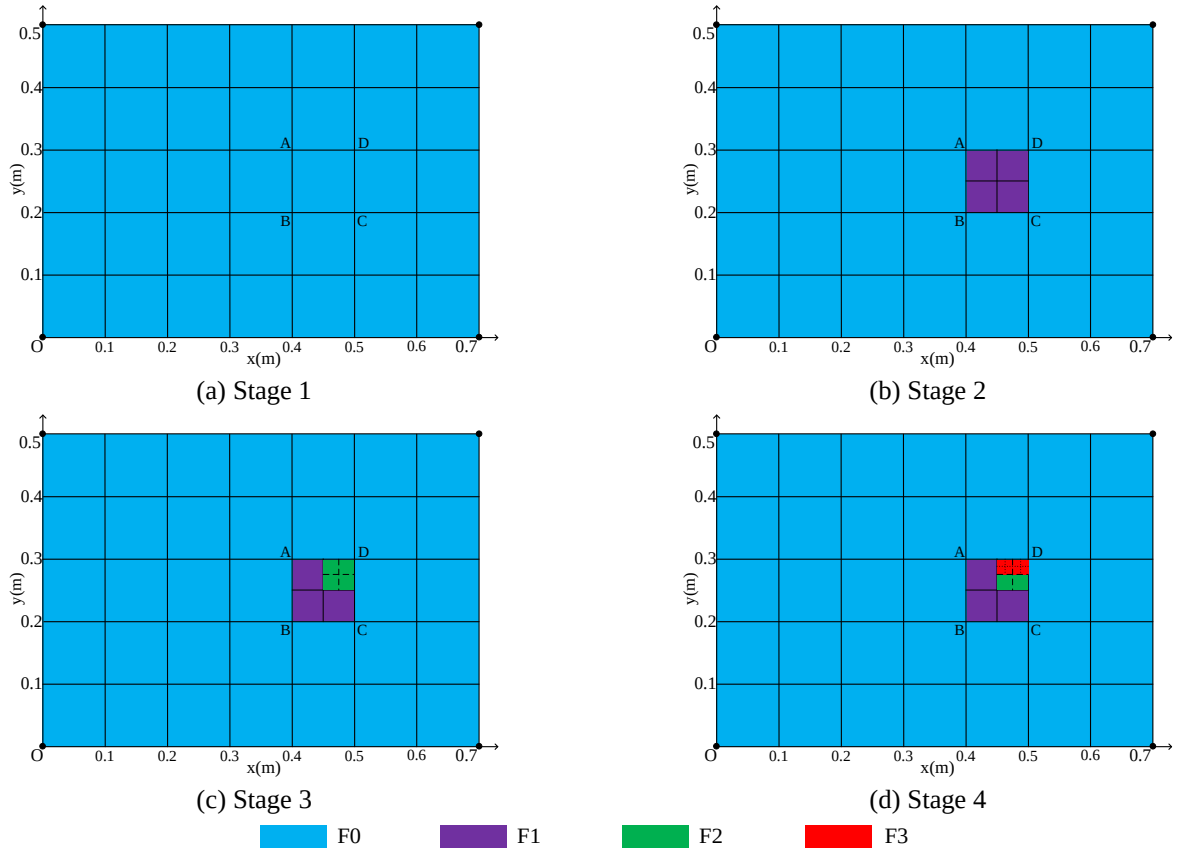

(a) Stage 1 (b) Stage 2

(c) Stage 3 (d) Stage 4

Fig. 4 Model refinement process in Case 1

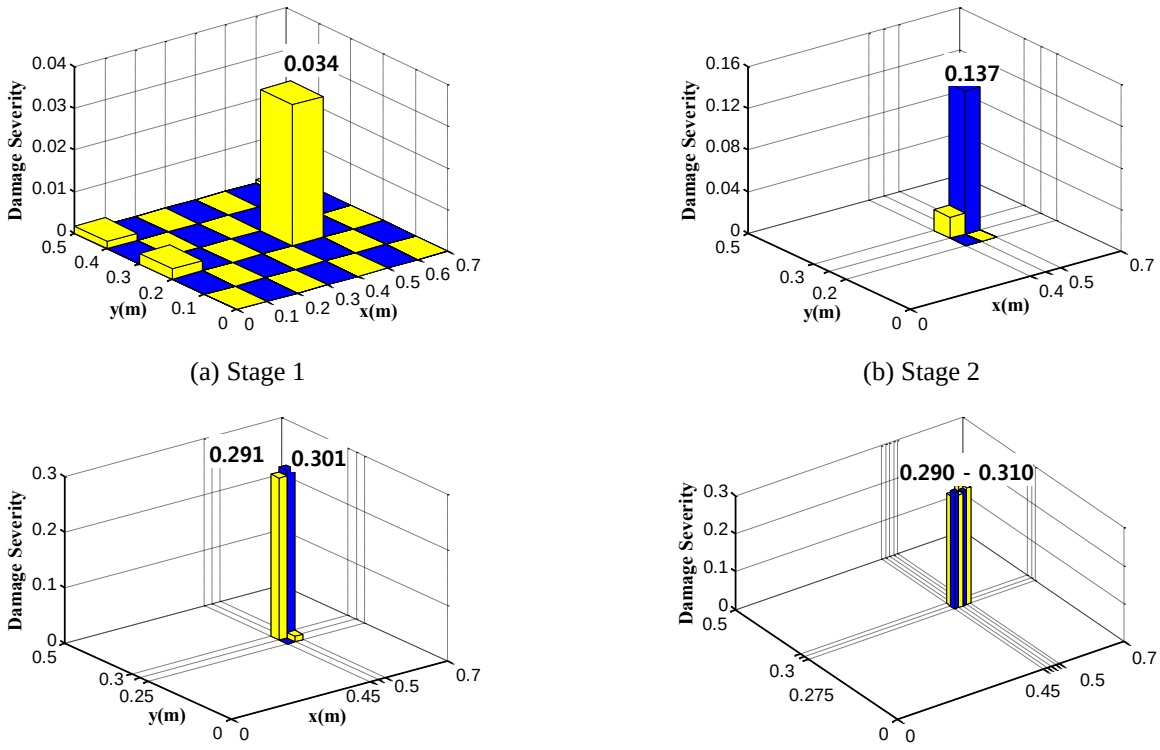

(a) Stage 1 (b) Stage 2

(c) Stage 3 (d) Stage 4

Fig. 5 Progressive damage detection results in Case 1

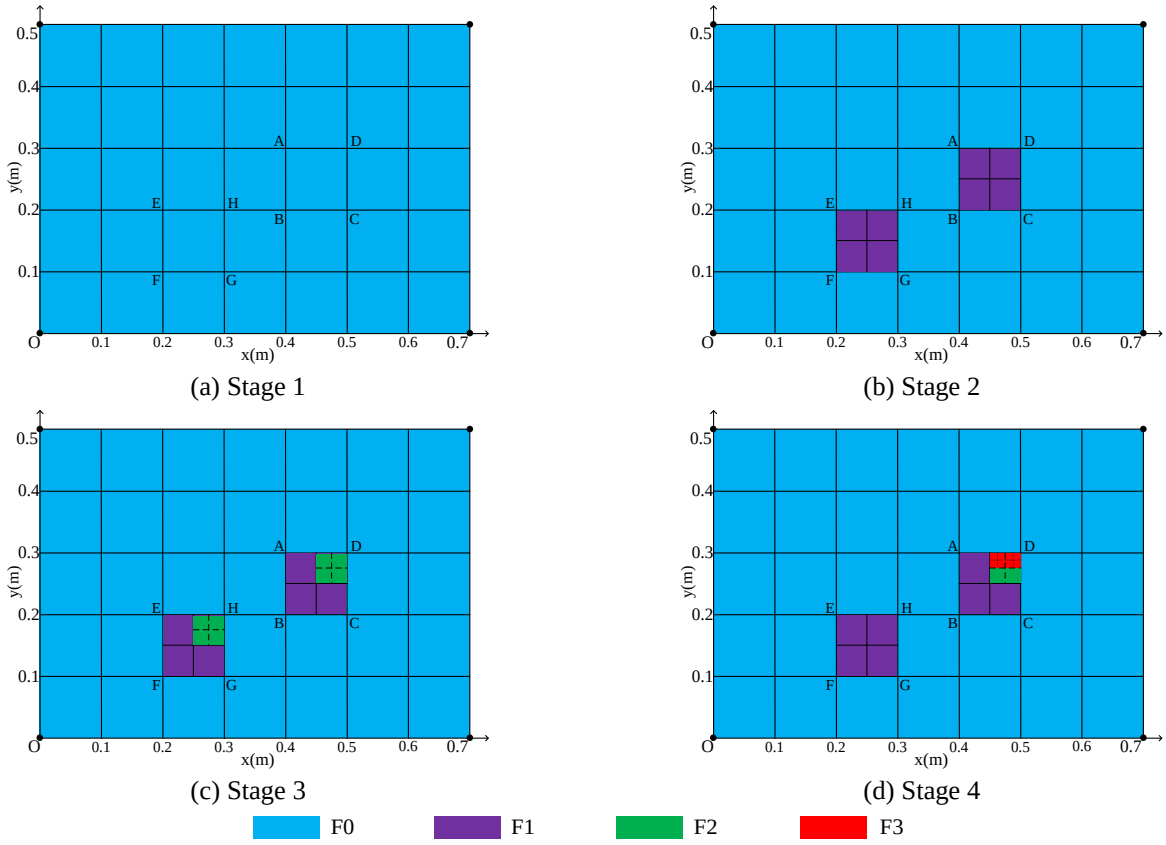

(a) Stage 1 (b) Stage 2

(c) Stage 3 (d) Stage 4

Fig. 6 Model refinement process in Case 2

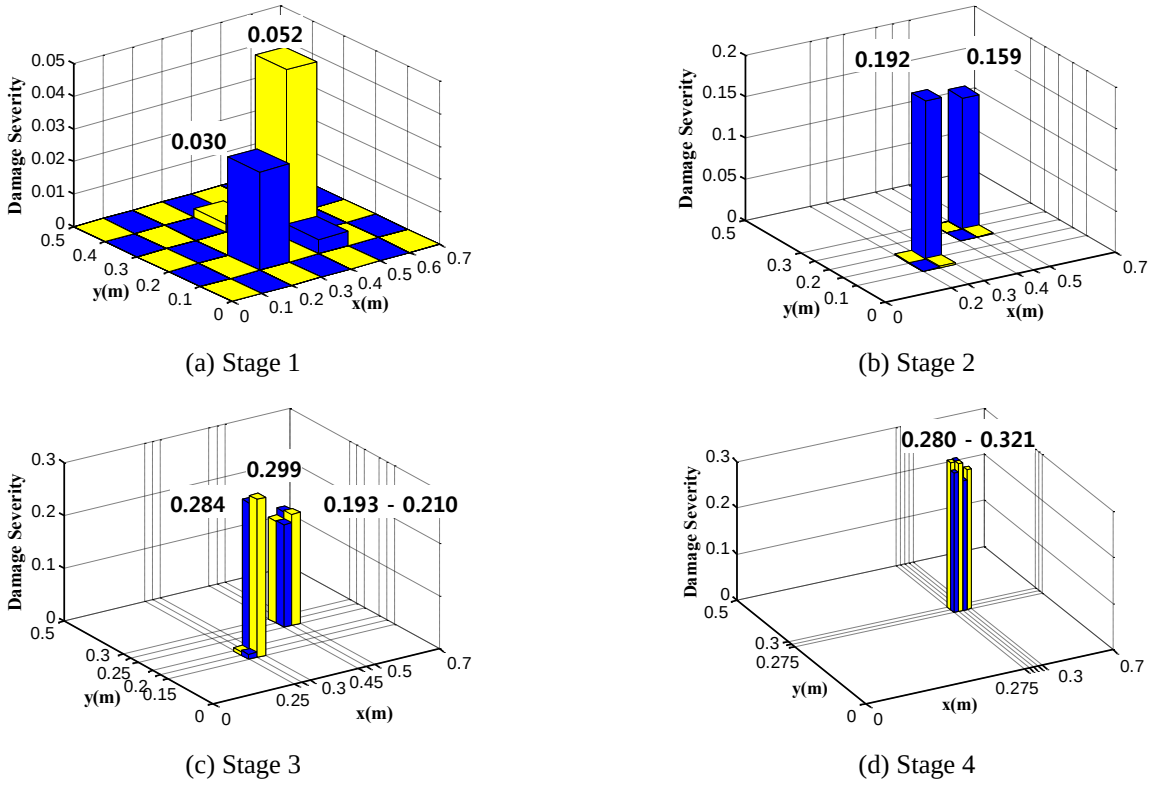

(a) Stage 1 (b) Stage 2

(c) Stage 3 (d) Stage 4

Fig. 7 Progressive damage detection results in Case 2

Table 2 Measurement locations effects

Damage scenario	No. of measured locations	Nodes	Results
1a	44	2-7,9-40,42,47	Success
1b	22	2,4,6,9,11,13,15,18,20,22, 24,25,	Success
1c	12	10,12,13,15,19,22, 27,30,34,36,37,39	Success
1d	8	10,12,13,15, 34,36,37,39	Fail

In view of this, no further refinement was conducted.

Fig. 6 shows the model refinement and updating process in Case 2, in which the plate was subject to double damages, that is, Damage I in [0.45, 0.5]×[0.275, 0.3] with 30% severity and Damage II in [0.35, 0.4]×[0.55, 0.6] with 20% severity, as listed in Table 1. Given that the extent of the two damages was not the same; this case highlighted the flexibility of WFEM in damage detection more clearly. The WFEM refinement process and damage detection results are presented in Figs. 6 and 7, respectively. Detection accuracy was effectively improved with the progressive refinement of WFEM. Unlike the Damage I, Damage II consisted of 1/140 (1/14×1/10) of the entire plate which was identified accurately in Stage 2 and verified in Stage 3. Then in Stage 4, the element scale related to this region ([0.25, 0.3]×[0.15, 0.2]) was reduced to the state as in Stage 2.

For model updating based damage detection methods, a large number of DOFs and updating parameters increase the computation amount and even make the solutions ill-conditioned and non-unique. As the WFEM scale can be adaptively adjusted according to actual damage, the structural damage can be identified with satisfactory accuracy only with the minimized number of DOFs in the model and updating parameters in optimization. For example, in Case 1, the numbers of DOFs in Stages 1 to 4 were 176, 180, 184, and 192, respectively; the corresponding numbers of updating parameters were 35, 4, 4, and 8, respectively. However, if traditional FEM is adopted, uniformly meshed 28×20 (at least 14×20) plate elements are required to accurately identify the damage because it consists of 1/280 (1/14×1/20) of the entire plate and cannot be known in advance. The numbers of DOFs and updating parameters will be 2,420 (at least 1,244) and 560 (at least 280), respectively. Thus, the optimization process would be impractical and time consuming, if not impossible. With the proposed method, damage detection becomes very efficient because only WFEM is refined in probable damage regions without the change of the sensor or measurement locations.

The number of measurement locations determines the amount of information available for model updating and thus affects the accuracy of the damage detection results to large extent. To investigate the effects of the measurement locations, Case 1 shown in Table 1 was re-analysed with different numbers of measurement locations. The number of measured nodes and the corresponding damage detection results are presented in Table 2. Considering the damage location is unknown in advance, the measurement locations are nearly uniformly distributed. Acceptable results could be obtained in this case when the number of the measurement locations was no less than 12. However, it is noteworthy that the least number of the required measurement locations is highly case-dependent, and influenced by damage scenarios, measurement noise levels, and so on.

5. Experimental study

5.1 Experiment description

Experiment of a thin aluminium plate with the dimensions of 405×455×3 mm^3 was conducted to examine the effectiveness of the proposed damage detection method in a real experimental environment. As shown in Fig. 8, two adjacent sides (right and lower edges) of the plate were clamped by two rigid beams with bolts and mounted on a testing table (NEWPORTs ST-UT2). Considering the great rigidity of the beams and the strong fastening capacity of the bolts, the boundary conditions of these two edges could be regarded as fixed ends. The physical material properties of the plate were: elastic modulus $E = 68.9$ Gpa , density $\rho = 2700$ Kg/m^3 , Poisson's ratio $\mu = 0.27$.

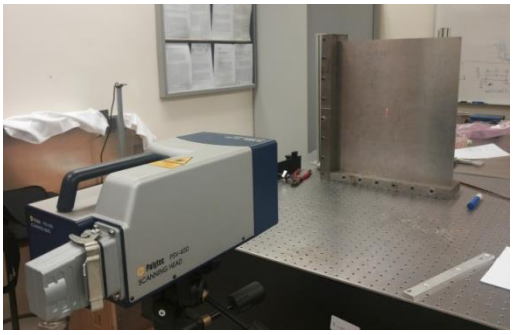

Fig. 8 Experiment set-up

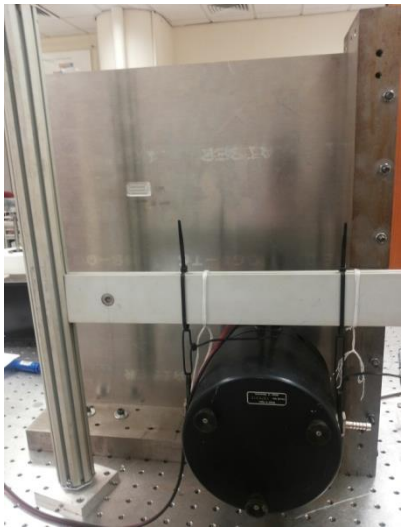

Fig. 9 Damage zone on the plate

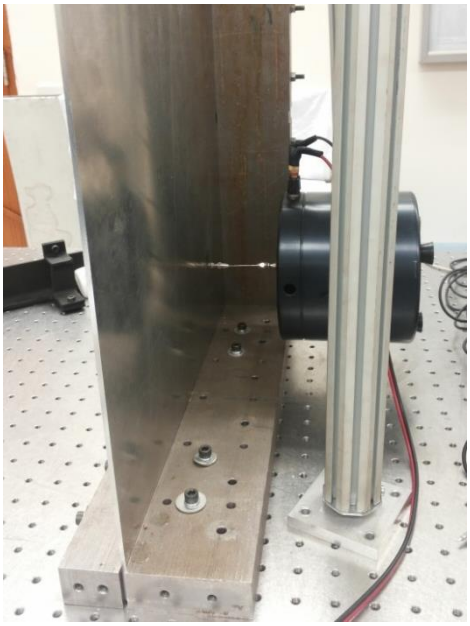

Fig. 10 Vibration exciter

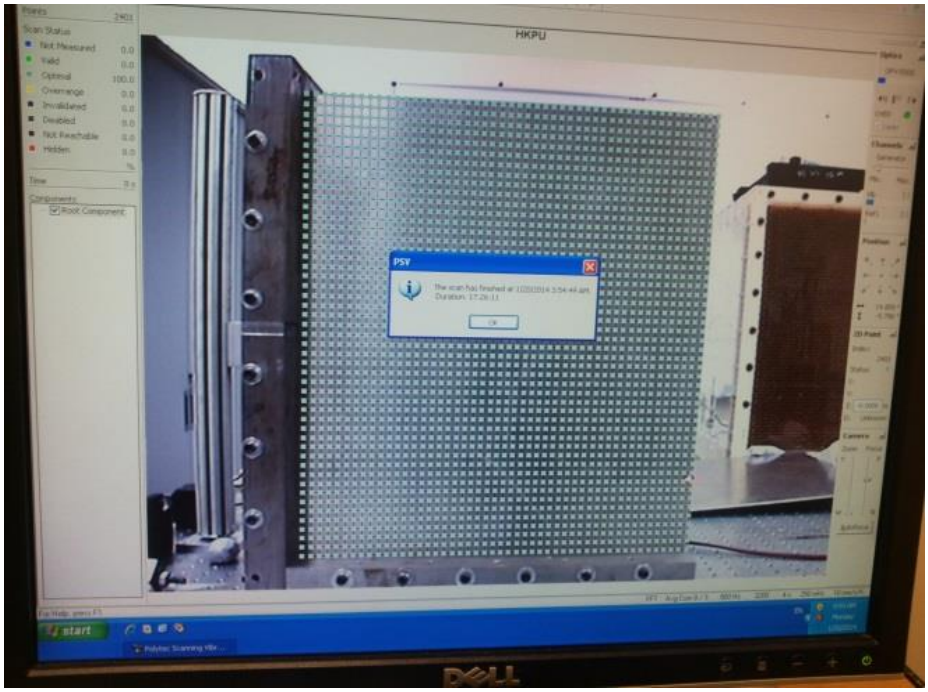

Fig. 11 Vibration test on the plate with 49×49 measurement points

Fig. 9 shows the damaged zone with the dimension of 32.7 mm × 18.4 mm. Thickness reduction of 2 mm was introduced by milling the plate. Given that the original thickness of the plate was 3 mm, damage severity (reduction in flexural rigidity) can be regarded as approximately 88.9%. An electro-mechanical exciter (B&Ks 4809, Fig. 10) was utilized to apply point-force excitation, and a scanning Doppler laser vibrometer system (Polytecs^{R} PSV-400) was employed to capture the out-of-plane displacements at each measurement point on the front surface of the plate. The system was non-contact, so there was no need to install sensors on the structure. It determined the operational deflection shapes and eigen modes as easily as taking a photograph. Besides, it can measure within fields-of-view from 1 mm×1 mm up to many square meters at a large measurement point density. However, high resolution measurement points will consume more scanning time.

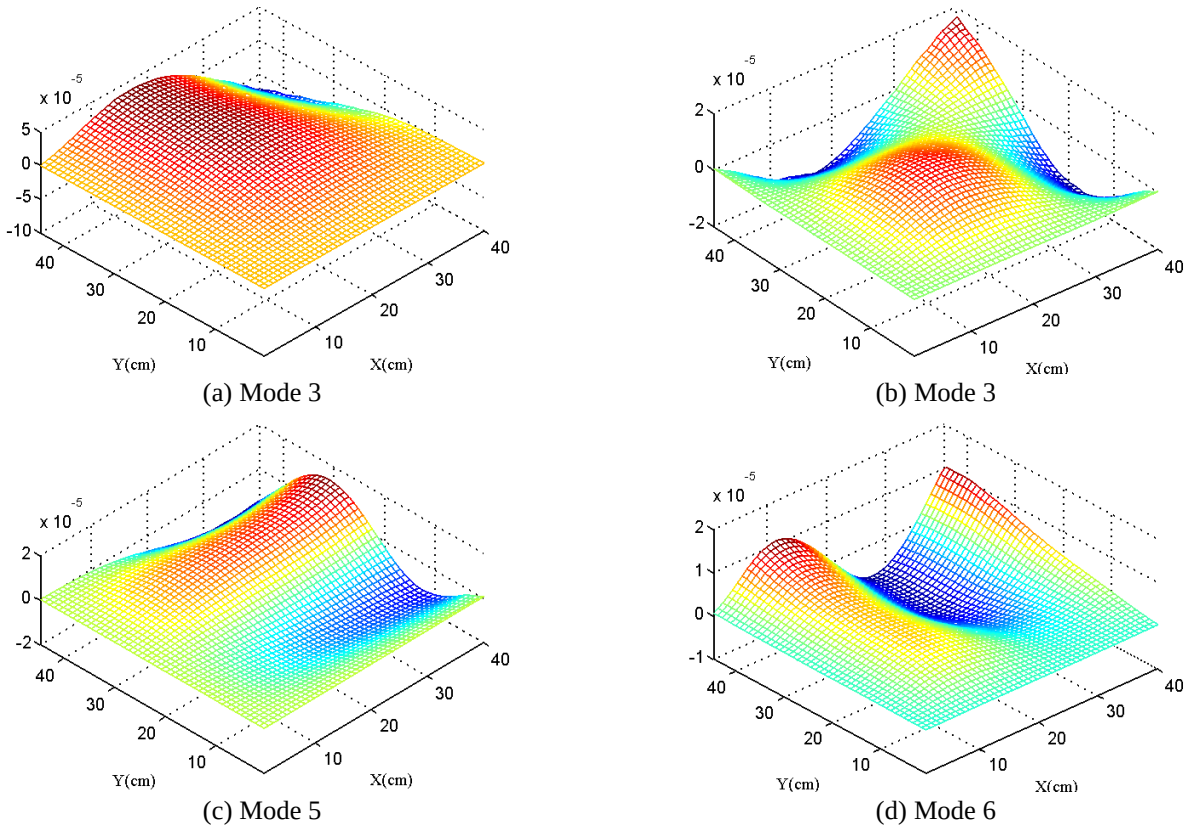

(a) Mode 3 (b) Mode 3

(c) Mode 5 (d) Mode 6

Fig. 12 Experimental mode shapes of the damaged plate

Based on the frequencies (Table 3) calculated from FEM of the plate in the undamaged state, the excitation frequency bands in the test are determined and listed in Table 3. Using narrow-band random excitation helps obtain high accuracy results. Single-input-single-output (excited at single point and measured at single point) was adopted in the vibration tests, and the test was repeated three times for each mode. Then, the average of the identified frequency values were regarded as the experimental frequencies of the plate in both undamaged and damaged states. The results are listed in Table 3.

In the following mode shape test, single-input-multi-output (excited at single point and measured at multi points) was adopted instead of single-input-single-output. Harmonic frequency excitation with a fixed frequency (e.g., 111.514 Hz for the third mode shape in the undamaged state) was used to excite the plate, and then the out-of-plane vibration displacements at the 49 × 49 discrete points were measured with the scanning Doppler laser vibrometer system (Fig. 11).

The displacement mode shape corresponding to this frequency was subsequently obtained. The mode shapes of the damaged plate are plotted in Fig. 12. The first and second vibration modes were not obtained because the electro-mechanical exciter was suspended and unable to reliably excite low-frequency vibration modes.

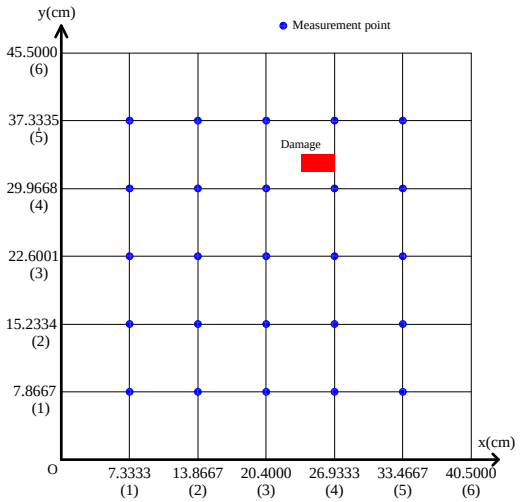

Fig. 13 Thin plate in the experimental study

Table 3 Frequencies of the plate in the experimental study (Hz)

Mode	FEM Value	Experimental Value		
	Undamaged	Excitation frequency	Undamaged	Damaged
3	109.885	[105, 115]	111.514	111.106
4	189.639	[185, 195]	189.870	189.544
5	227.818	[225, 235]	233.161	232.263
6	281.531	[275, 285]	282.359	281.232

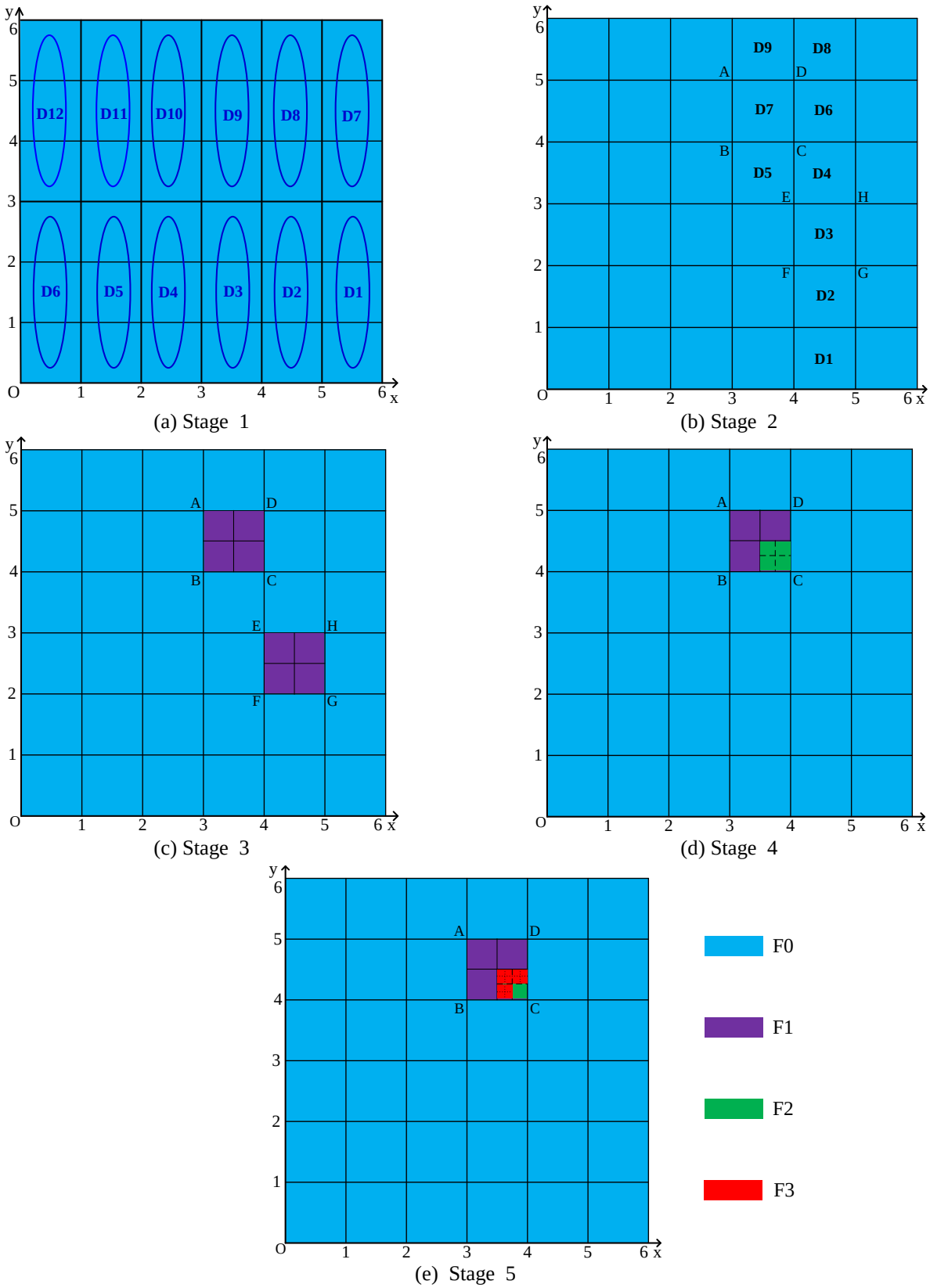

(a) Stage 1

(b) Stage 2

(c) Stage 3

(d) Stage 4

(e) Stage 5

Fig. 14 Model refinement process in the experiment study

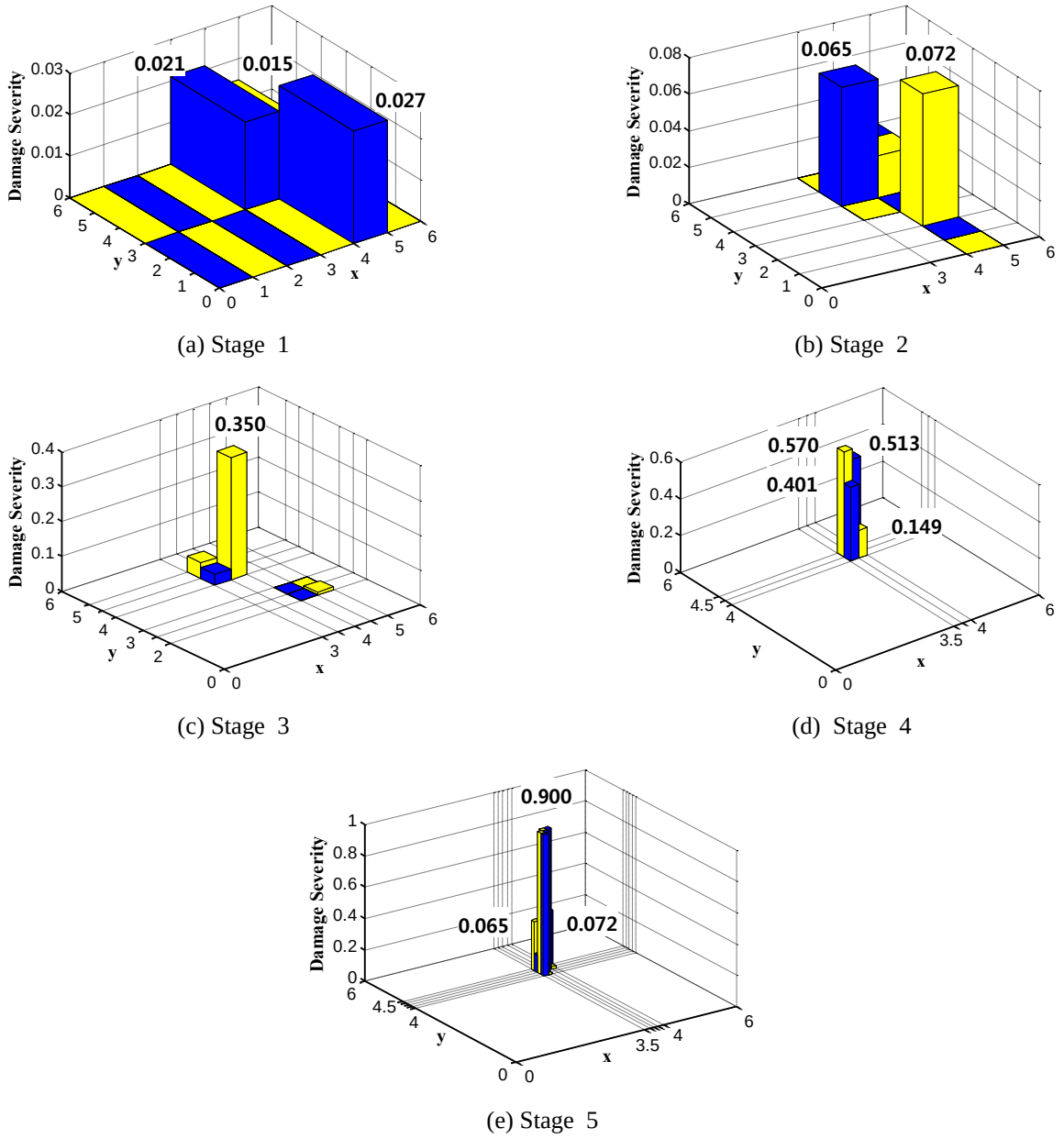

(a) Stage 1 (b) Stage 2

(c) Stage 3 (d) Stage 4

(e) Stage 5

Fig. 15 Progressive damage detection results of the plate experiment

5.2 Damage detection

The frequencies and MACs corresponding to the 3rd to 6th modes were used in the damage detection process. Although 49×49 spaced points were acquired in the experiment, only data at 5×5 points are used in damage detection considering the fact that too dense measurement in vibration tests require many sensors and increase the demand for signal acquisition, transmission, and processing, which may not be practical in the vibration tests of civil structures. In WFEM, the plate was initially divided into 6×6 wavelet plate elements, as show in Fig. 13.

The original dimensions of the elements were not uniform to make the nodes of the elements consistent with the 25 measurement points. For simplicity, the dimensions of the plate shown in Fig. 13 were normalized to [0, 6] × [0, 6] so that all the 36 elements are represented by a square with unit dimensions.

Too many updating parameters often cause difficulty in damage detection, particularly with the presence of test noise or other environmental factors. To further reduce the number of updating parameters in the initial stage, only 12 flexural rigidities (i.e., D1, D2 …… D12) as shown in Fig. 14(a) were selected for update in Stage 1. In other words, every three elements were assumed to have a uniform parameter. The updating results are shown in Fig. 15(a). The elements related to D2, D8, and D9 were identified as possible damage regions. In Stage 2, the flexural rigidities of nine elements (Fig. 14(b)) were selected as updating parameters, and the optimization process was performed

again.

The results showed that the regions [3, 4] × [4, 5] (denoted as ABCD) and [4, 5] × [2, 3] (denoted as EFGH) were possible damage regions. Further refinements in these two regions were made in the following procedures. Figs. 14(c) and 15 show the damage detection process and the corresponding results, respectively. Although misjudgement occurred in the beginning stage of the damage detection process, accuracy was improved gradually with the refinement of WFEM. In Stage 4, the damages were located in three regions, namely, [3.5, 3.75] × [4, 4.25], [3.5, 3.75] × [4.25, 4.5], and [3.75, 4] × [4.25, 4.5], but the third region was a misjudgement. The damage severities were fairly satisfactory albeit different from the real value (0.89) although the third region was a misjudgement. Further refinement in Stage 5 improved the damage detection results in terms of damage severity.

6. Discussion

Boundary conditions affect modal properties and may influence damage detection accordingly. In this study, two examples with different boundary conditions (simply supported and fixed boundaries) were considered in the numerical and experimental cases. The proposed damage detection method performed well in both cases. Notably, both fixed and simply supported conditions are ideal boundary conditions. Actual boundary conditions can be flexible or semi-rigid rather than perfectly fixed or simply supported conditions. Consequently, in the WFEM updating process, the support stiffness coefficients should be included as the updating parameters, in addition to flexural rigidities of plates. Both the support stiffness parameters and damage indices should be obtained via optimization. Moreover, modal properties measured in a real structure inevitably involve uncertainties, which may influence the performance of modal property-based damage detection methods. The impact of such uncertainties needs to be quantified by using the Bayesian modal identification methods (Au *et al*. 2013).

7. Conclusions

The FEM updating technique is widely and successfully used in damage detection. However, when applied to plate structures, the traditional FEM updating may result in a large number of DOFs in structural model and updating parameters in optimization, which causes the difficulty in damage detection. In view of this, a WFEM-based progressive damage detection method which is efficient in terms of DOFs and updating parameters was applied to thin plate structures. The multi-scale eigenvalue equation for obtaining the modal parameters of thin plate structures was derived with the tensor product of cubic Hermite multi-wavelets as elemental shape functions. Then the procedure for detecting sub-element damage gradually through updating the multi-scale WFEM with an objective function combining frequencies and MACs was developed. The scale of the wavelet elements in the regions of concern could be adaptively enhanced or reduced to remain comparable with gradually identified damage scenarios. The test modal information remained the same, that is, no measurement point movement or addition was required.

Numerical and experimental examples were investigated with different damage scenarios to demonstrate the effectiveness of the proposed method. The results indicated that compared with traditional FEM, the proposed method can identify structural damage with satisfactory accuracy and with reduced numbers of DOFs in the model and updating parameters in the optimization. Although sometimes misjudgements occur during the detection process, further refining the WFEM in the subsequent stages would lead to high accuracy and successfully remove the initial false alarms.

In this study, model updating technique was adopted to detect damage. Its success depends on the accuracy of FEM, definition of optimization problem, and selection of the optimization algorithm. Although this study was focused on structural modeling, the latest advances in model updating technique may be further introduced to improve the performance of the WFEM-based damage detection method.

Acknowledgements

The authors are grateful for the financial support from the National Key Research and Development Program of China (NO. 2016YFC0701400), National Science Foundation of China (Project No. 51878234 and 51778550), and from The Hong Kong Polytechnic University (Project No. G-YBHK). The authors would like to thank Dr. Zhongqing Su and Dr. Hao Xu from The Hong Kong Polytechnic University for their help in the plate vibration testing. Findings and opinions expressed here, however, are those of the authors alone, not necessarily the views of the sponsors.

References

Amaratunga, K. and Sudarshan, R. (2006), "Multi-resolution modeling with operator-customized wavelets derived from finite elements", *Comput. Method. Appl. M.*, **195**, 2509-2532.

Antonio, J.G.P. and Erin, S.B. (2014), "Structural model updating using dynamic data", *J. Civil. Struct. Health Monit.*, **4**(3), 177-194.

Au, S.K., Zhang, F.L. and Ni, Y.C. (2013), "Bayesian operational modal analysis: theory, computation, practice", *Comput. Struct.*, **126**, 3-14.

Bayissa, W.L. and Haritos, N. (2007), "Damage identification in plate-like structures using bending moment response power spectral density", *Struct. Health Monit.*, **6**, 5-24.

Becker, R. and Braack, M. (2000), "Multigrid techniques for finite elements on locally refined meshes", *Numer. Linear. Algebr.*, **7**, 363-379.

Beheshti-Aval, S.B., Taherinasab, M. and Noori, M. (2011), "Using harmonic class loading for damage identification of plates by wavelet transformation approach", *Smart Struct. Syst.*, **8**(3), 253-274.

Biboulet, N., Gravouil, A., Dureisseix, D., Lubrecht, A.A. and Combescure, A. (2014), "An efficient linear elastic FEM solver using automatic local grid refinement and accuracy control", *Finite Elem. Anal. Des.*, **68**, 23-38.

Bogner, F.K., Fox, R.L. and Schmit, L.A. (1995), "The generation of interelement, compatible displacement stiffness and mass matrices by the use of interpolation formulae", Proc FCMMSM 1995, Air Force Flight Dynamics Laboratory, Wright Patterson Air Force Base.

Cornwell, P., Doebling, S.W. and Farrar, C.R. (1999), "Application of the strain energy damage detection method to plate-like structures", *J. Sound Vib.*, **224**(2), 359-374.

Diaz, L.A., Martin, M.T. and Vampa, V. (2009), "Daubechies wavelet beam and plate finite elements", *Finite Elem. Anal. Des.*, **45**(3), 200-209.

Fan, W. and Qiao, P.Z. (2011), "Vibration-based damage identification methods: a review and comparative study", *Struct. Health Monit.*, **10**(1), 83-111.

Fan, W. and Qiao, P.Z. (2012), "A strain energy-based damage severity correction factor method for damage identification in plate-type structures", *Mech. Syst. Signal Pr.*, **28**, 660-678.

Fang, S.E., Perera, R. and Roeck, G.D. (2008), "Damage identification of a reinforced concrete frame by finite element model updating using damage parameterization", *J. Sound Vib.*, **313**, 544-559.

Fu, Y.Z, Lu, Z.R. and Liu, J.K. (2013), "Damage identification in plates using finite element model updating in time domain", *J. Sound Vib*., **332**, 7018-7032.

Han, J.G., Ren, W.X. and Huang, Y. (2006), "A spline wavelet finite-element method in structural mechanics", *Int. J. Numer. Meth. Eng.*, **66**, 166-190.

He, W.Y. and Ren, W.X. (2012), "Finite element analysis of beam structures based on trigonometric wavelet", *Finite Elem. Anal. Des.*, **51**, 59-66.

He, W.Y. and Ren, W.X. (2013), "Trigonometric wavelet-based method for elastic thin plate analysis", *Appl. Math. Model.*, **37**, 1607-1617.

He, W.Y. and Zhu, S. (2013), "Progressive damage detection based on multi-scale wavelet finite element model: numerical study", *Comput. Struct.*, **125**, 177-186.

He, W.Y. and Zhu, S. (2014), "Adaptive-scale damage detection strategy for plate structures based on wavelet finite element model", *Struct. Eng. Mech.*, **54**(2), 239-256.

He, W.Y., Zhu, S. and Ren, W.X. (2014), "A wavelet finite element-based adaptive-scale damage detection strategy", *Smart Struct. Syst.*, **14**(3), 285-305.

Hu, H. and Wu, C. (2009), "Development of scanning damage index for the damage detection of plate structures using modal strain energy method", *Mech. Syst. Signal Pr.*, **23**, 274-287.

Jaishi, B. and Ren, W.X. (2005), "Structural finite element model updating using ambient vibration test results", *J. Eng. Mech.-ASCE*, **131**(4), 617-628.

Kazemi, S., Fooladi, A. and Rahai, A.R. (2010), "Implementation of the modal flexibility variation to fault identification in thin plates", *Acta Astronaut*, **66**, 414-426.

Lee, U. and Shin, J. (2002), "A structural damage identification method for plate structures", *Eng. Struct.*, **24**, 1177-1188.

Li, B. and Chen, X.F. (2014), "Wavelet-based numerical analysis: a review and classification", *Finite Elem. Anal. Des.*, **81**, 14-31.

Quraishi, S.M. and Sandeep, K. (2013), "Multiscale modeling of beam and plates using customized second-generation wavelets", *J. Eng. Math.*, **83**, 185-202.

Rucka, M. and Wilde, K. (2006), "Application of continuous wavelet transform in vibration based damage detection method for beams and plates", *J. Sound Vib.*, **297**, 536-550.

Teughels, A., Maeck, J. and Roeck, G.D. (2002), "Damage assessment by FE model updating using damage functions", *Comput. Struct.*, **80**(25), 1869-1879.

Wang, Y.M. and Wu, Q. (2013), "Construction of operator-orthogonal wavelet-based elements for adaptive analysis of thin plate bending problems", *CMES-Comp Model. Eng.*, **93**(1), 17-45.

Wu, D. and Law, S.S. (2004), "Damage localization in plate structures from uniform load surface curvature", *J. Sound Vib.*, **276**, 227-244.

Xiang, J.W., Chen, X.F., He, Z.J. and Zhang, Y.H. (2008), "A new wavelet-based thin plate element using B-spline wavelet on the interval", *Comput. Mech.*, **41**(2), 243-255.

Yam, L.H., Li, Y.Y. and Wong, W.O. (2002), "Sensitivity studies of parameters for damage detection of plate-like structures using static and dynamic approaches", *Eng. Struct.*, **24**, 1465-1475.

Yan, Y.J., Cheng, L., Wu, Z.Y. and Yam, L.H. (2007), "Development in vibration-based structural damage detection technique", *Mech. Syst. Signal Pr.*, **21**, 2198-2211.

Zhu, S., He, W.Y. and Ren, W.X. (2013), "Adaptive-scale damage detection for frame structures using beam-type wavelet finite element: experimental validation", *J. Earthq. Tsunami*, **7**(3), 1350024.

FC